A Framework for Comparing and Predicting Stirrer Efficiencies in Different Reverberation Chambers

Andréa Cozza

A Framework for Comparing and Predicting Stirrer Efficiencies in Different Reverberation Chambers

Andrea Cozza, *Senior Member, IEEE*

***Abstract*—The concept of stirring coherence time has been recently introduced as an effective way of measuring the ability of a mechanical stirrer to introduce disorder in a reverberation chamber (RC) and predicting the stirrer efficiency under any loading condition. This paper builds upon those findings by introducing the intrinsic stirrer efficiency parameters (ISEP), which are independent of the RC features. Tests in three different RCs confirm the viability of this approach, with several practical implications for RC users. First, the ISEP clarify why a stirrer with good efficiency in an RC will display a lower efficiency in a larger RC, explaining in quantitative terms why a larger stirrer is often necessary if a target stirring efficiency is required. Second, a stirrer can be characterized in any RC, obtaining the same ISEP, thus allowing a direct comparison of the performance of different stirrer designs, unbiased by the RC features, simplifying the identification of the main physical mechanisms responsible for the stirring efficiency. Finally, since the ISEP can predict a stirrer efficiency in other RCs, an optimal stirrer design can be straightforwardly selected from the ISEP of previously tested stirrers, avoiding renewed testing of multiple stirrer prototypes.**

***Index Terms*—Reverberation chambers, mechanical stirrers, stirring efficiency, auto-correlation function, stirrer design.**

I. Introduction

MECHANICAL stirrers are fundamental devices used in reverberation chambers (RC), where they introduce variable boundary conditions, in order to create ideally independent and complementary electromagnetic testing environments [1]. In practice, only a fraction of these configurations can be regarded as independent, which represents the stirring efficiency provided by the stirrer. In this respect, an inefficient stirrer can limit the lowest usable frequency, or LUF, for which an RC can be regarded as compliant to EMC test standards such as [2], [3]. A common way of assessing the stirring efficiency is based on the auto-correlation function (ACF) between field or power samples measured in the RC, collected for different stirrer positions [2], [4].

The important role played by stirrers in RC testing has spurred multiple investigations searching for guidelines for an optimal design, overwhelmingly driven by experimental or numerical results. A wide body of works in the literature has investigated how the stirring efficiency depends on the stirrer electrical dimensions and shape, resulting in the proposal of diverse solutions with potentially complex shapes [5]–[18].

In fact, experimental evidence over the years has indicated that the stirrer design is not the only reason for a limited efficiency: several papers have highlighted that a higher RC loading systematically results in a loss of efficiency [19]–[26], as well as the fact that increasing an RC volume also results in a lower efficiency [9].

A recent paper has introduced a model quantitatively explaining how losses hinder the stirring efficiency [27], by means of two time constants: the power-decay time τ_a, measuring the average rate of loss in an RC and the stirring coherence time τ_s, which measures the rate of disorder introduced by changing the stirrer position. Maximum loading conditions ensuring an acceptable stirrer efficiency are discussed in [27] and have a direct bearing on the LUF.

A direct consequence of that model is that it would be wrong to compare the efficiency of different stirrer designs by means of their ACF, since they also depend on the power loss in the RC where they were respectively tested. Therefore, a stirrer design deemed optimal for a given RC may not perform as well in another RC with different features (volume, surface, conductivity, loading, etc.) , making it hard to compare results obtained in independent investigations and draw conclusions about optimal stirrer design guidelines.

This paper explores how this stirring efficiency model can be used in order to define a framework for comparing the stirring performance of mechanical stirrers tested in different RC settings, avoiding biases introduced by the differences in volume and loading conditions. We first recall in Sec. II the main results from [27] and how they naturally provide a simple framework to compare stirrer efficiencies. The experimental setup used for validating this idea is described in Sec. III, based on stirrer testing across three different RCs. Independence from the RC configuration is proven in Sec. IV, setting the ground for the direct comparison of different stirrer designs. Extensive results are presented in Sec. V, based on more than 30 stirrer designs with different shapes and dimensions, tested over a wide frequency range, providing clear evidence that for electrically large stirrers the main mechanism behind stirring efficiency is surface scattering. Sec. VI proves that the proposed framework can also be applied to predict how a stirrer's efficiency changes when moved to an RC with different features. This property provides a simple, fast and accurate tool for selecting the most suitable stirrer design for a given RC, out of a library of previously tested stirrer models. Finally, Sec. VII uses this result to show that in order to ensure the same stirring efficiency, larger RCs require a larger stirrer, thus compensating for higher losses over their larger metallic surface. At the same time, these results also prove that design rules focusing on the ACF are not sufficient to ensure a target stirring efficiency, since they do not take into account the impact of power loss.

A. Cozza is with the Group of Electrical Engineering - Paris (GeePs), CentraleSupelec, Univ. Paris-Sud, Université Paris-Saclay, Sorbonne Universités, UPMC Univ Paris 06, 3 & 11 rue Joliot-Curie, Plateau de Moulon 91192 Gif-sur-Yvette CEDEX, France (email: andrea.cozza@ieee.org).

II. Stirring Correlation

The stirring efficiency of mechanical stirrers is typically measured by means of the ACF between field samples acquired by a field probe, collected for each position of the stirrer. Alternatively, the output signal of a receiving antenna, or the received power can be used [2]. Since harmonic steady-state conditions are applied during these tests, this frequency-domain version of the ACF will be referred to as fACF and noted as $R(\nu;k)$, for a frequency ν and lag k, defined as

$$R(\nu;k)=\frac{\langle x^{\star}(\nu;\psi)x(\nu;\psi_k)\rangle_{\psi}}{\left\langle|x(\nu;\psi)|^2\right\rangle_{\psi}} \tag{1}$$

with $x(\nu;\psi)$ the field sample measured for a stirrer position ψ, assuming that $x(\nu)$ has already been zero-averaged; $\psi_k=\psi+k\Delta\psi$ with $\Delta\psi$ the stirrer rotation step. Brackets represent the average through the entire set of samples collected at each stirrer position. The lag dependence will be mostly dropped in the rest of this paper, for the sake of compactness.

An alternative approach for estimating the fACF was introduced in [27], where the effect of mechanical stirrers was revisited in time domain. Here, stirrers progressively introduce disorder in an RC, with an increasingly large loss of coherence between the results observed for two different stirrer positions. This behavior can be measured by first computing the ACF in time domain (tACF), from the narrow-band responses centered at the frequency f_c, as defined in (2). A model inspired by transport theory, supported by extensive experimental results, proved that the tACF obeys a decaying exponential function

$$R(t;f_c,k)=\frac{\langle x^{\star}(t;f_c,\psi)x(t;f_c,\psi_k)\rangle_{\psi}}{\left\langle|x(t;f_c,\psi)|^2\right\rangle_{\psi}}=R_s\mathrm{e}^{-t/\tau_s}, \tag{2}$$

where $\tau_s(f_c,k)$ is the stirring coherence time, measuring the rate of loss of coherence introduced by the stirrer, while $R_s(f_c,k)$ measures the early-time coherence loss introduced by the first few interactions of the stirrer with the wavefront radiated by the antenna [27]. R_s is important since it describes the fACF expected under heavy loading conditions. The stirring coherence time should not be confused with the stirrer damping time [28], which measures the rate of diffusion introduced by a stirrer, instead of the loss of coherence caused by a stirrer changing position.

As proven in [27], once R_s and τ_s in (2) are know, it is possible to predict the fACF from knowledge of the RC power-decay time $\tau_a=Q/2\pi f_c$, where Q is the composite average quality factor,

$$R(f_c)=\frac{R_s(f_c)}{1+\tau_a(f_c)/\tau_s(f_c)}. \tag{3}$$

According to (3) the fACF is mostly controlled by the ratio τ_a/τ_s, with $R(f_c)\ll 1$ as $\tau_a/\tau_s\gg 1$, i.e., for a slow power decay, comparatively to the rate of disorder introduced by the stirrer, measured by τ_s. If an RC is expected to be used under higher loading conditions, the stirrer efficiency can be guaranteed only by using a stirrer with a smaller τ_s, i.e, if it introduces disorder in a shorter time. This model was applied in [27] in order to predict how the fACF degrades under increasingly loaded conditions, with the stirrer parameters R_s and τ_s proven to be independent of the RC loading.

In the following sections this model is applied to a more general problem, where a stirrer efficiency needs to be predicted for an RC different from the one where it was initially tested, e.g., with a different volume. This requires that the stirrer parameters be RC independent, not only with respect to loading conditions, but also its dimensions. In fact, a by-product of the transport-theory model introduced in [27] is the prediction that τ_s must be directly proportional to the RC volume V, as

$$\tau_s=V\tau_o. \tag{4}$$

Therefore, it can be surmised that when a stirrer is used in RCs of different volume, τ_s would be modified, with the larger RC requiring longer times in order for the stirrer to introduce disorder. This important property is confirmed in Sec. IV and its consequences on the fACF are discussed in Secs. VI and VII.

The parameters τ_o and R_s are now both independent of volume and loading conditions and will therefore be referred to as intrinsic stirrer efficiency parameters (ISEP). This property implies that the performance of different stirrers measured in different RCs could be directly compared, instead of relying on the fACF, which heavily depends on their volume and loading conditions. Moreover, having estimated τ_o in a given RC, it should also be possible to predict the fACF it would warrant if used in another RC, with a different volume and losses, as according to (3).

TABLE I: Main features of the three RCs used during experiments and the stirrer cases tested therein (cf. Table II).

RC	dimensions (m^3)	volume (m^3)	surface (m^2)	metal	#
A	$0.750\times 1\times 1.06$	0.795	5.21	alum.	1-8, 23,25,31
B	$0.750\times 1\times 1.98$	1.49	8.43	alum.	1-34
C	$3.08\times 1.85\times 2.45$	14.0	35.6	galv. steel	1-12

III. Experimental Setup and Data Processing

In order to confirm that the ISEP are independent of the RC where a stirrer is tested, experimental investigations were carried out in three different RC settings, described in Table I, based on the two facilities shown in Fig. 1. The first RC, with walls made of an aluminium alloy, is a reconfigurable cavity with a movable shelf allowing to easily modify the cavity height and volume. Two configurations were thus considered, with a 0.795 m^3 and a 1.485 m^3 volume, respectively. The second RC was based on galvannealed steel plates, with a 13.9 m^3 volume. These three configurations will be respectively referred to as RC A, B and C in the following.

Several stirrers were tested in the three RCs, over 100 stirrer steps. The same monocone antenna, visible in Fig. 1, was used for exciting the RCs over ten thousand frequency samples between 0.6 and 6 GHz, measuring the S_{11} at the input port of the cable feeding the antenna, by means of an E8363B

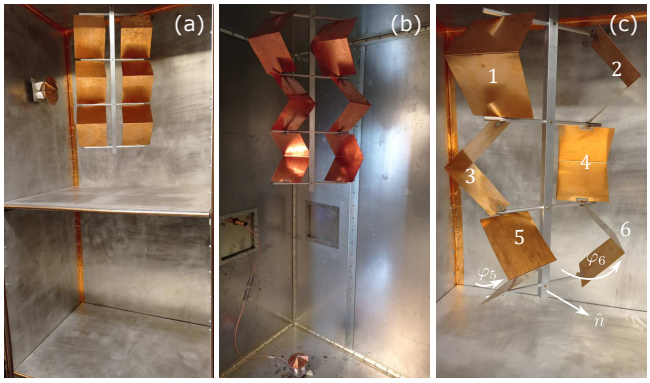

Fig. 1: The three RCs used in the experimental validation of the proposed method: (a) aluminium-based reconfigurable RC (cases A and B); (b) galvannealed steel-based RC (case C). The notation for the orientation of the stirrer elements is given in (c).

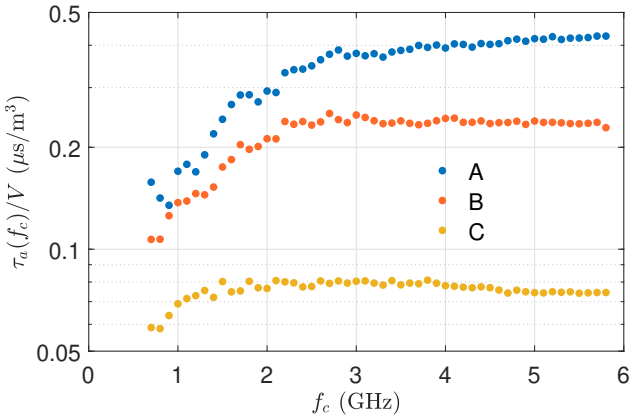

Fig. 2: Power-decay time τ_a estimated for the three RCs described in Table I, normalized to the their respective volumes.

Agilent vector network analyzer. The antenna free-space S_{11} was better than -6 dB over the test frequency range and was used as a baseline, in order to isolate the RCs responses.

Each test involved post-processing the baselined S_{11} results in order to estimate the tACF, as defined in (2), for a central frequency f_c varying from 0.7 to 5.8 GHz in 0.1 GHz steps. For each value of f_c the frequency samples recorded over a 5 % relative bandwidth were processed through an FFT in order to recover the narrow-band time-domain responses of the RC required by (2).

A least-square regression towards a decaying exponential was then applied to the tACF, in order to estimate R_s and τ_s. This operation differs from standard least-square regressions because the tACF estimate derived from a population of 100 stirrer steps is affected by a statistical uncertainty that cannot be modeled as a stationary Gaussian noise. In fact, the sample probability distribution of a correlation coefficient widely varies depending on the underlying correlation value: high correlation values have a very small uncertainty, even for small sample sizes, whereas low correlation values come with a much larger uncertainty even for large sample populations [29]. It is therefore necessary, before proceeding to the data regression, to identify the interval of the tACF presenting values within the confidence interval for a zero correlation. Indeed samples within this interval would mostly contribute maximum statistical uncertainty. For a 100 stirrer sample population the 95 % confidence interval is approximately $[-0.2, 0.2]$ [29]. The regression was then based only on the tACF samples occurring before the tACF enters this region.

The power-decay time τ_a was also estimated from S_{11} data, based on the power-delay profile [30], as it is needed for predicting the fACF in (3). Results for τ_a versus frequency are shown in Fig. 2, normalized to the respective RC volumes. The values of τ_a for RC A and B asymptotically scale as the ratio of the area of their boundary surfaces, indicating that losses are mostly driven by dissipation by the metallic boundaries.

Multiple stirrer designs were tested within the three RCs. They were created by rotating or removing part of the six dihedral elements of the stirrer shown in Fig. 1(c), each made

TABLE II: STIRRER CONFIGURATIONS TESTED DURING THE EXPERIMENTS. THE SIX ANGLES φ_i ARE DEFINED AS IN FIG. 1, WITH AN HYPHEN INDICATING THAT A DIHEDRAL ELEMENT WAS REMOVED.

#	φ_1	φ_2	φ_3	φ_4	φ_5	φ_6	
1	0	0	0	0	0	0	6 elements
2	0	0	180	180	0	0	
3	0	45	0	45	0	45	
4	0	90	0	90	0	90	
5	-45	-45	45	45	-45	-45	
6	180	0	-45	45	0	180	
7	135	135	-135	-135	-45	-45	
8	135	-135	-135	135	-45	45	
9	45	45	45	45	45	45	
10	-45	45	-45	45	-45	45	
11	-45	45	45	-45	-45	45	
12	45	45	-135	-135	45	45	
13	-45	45	-45	45	-	-	4 elements
14	-45	-45	45	45	-	-	
15	45	45	45	45	-	-	
16	45	45	-135	-135	-	-	
17	-45	-45	-	-	45	45	
18	45	45	-	-	-135	-135	
19	-	-	-45	-45	45	45	
20	-	-	45	45	-135	-135	
21	45	-	45	-	45	-	3 el.
22	45	-	-135	-	45	-	
23	-45	-45	-	-	-	-	2 elements
24	-	-	-45	-45	-	-	
25	-	-	-	-	-45	-45	
26	-45	-	-45	-	-	-	
27	-	-	-45	-	-45	-	
28	-45	-	-	-	-45	-	
29	-	-45	-	-	-45	-	
30	-	-	-	-45	-45	-	
31	-45	-	-	-	-	-	1 el.
32	-	-	-45	-	-	-	
33	-	-	-	-	-45	-	
34	-	-	-	-	-	-	

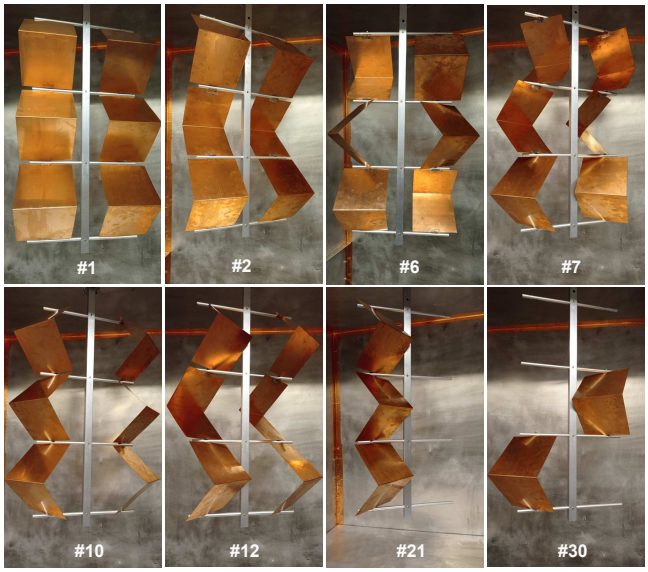

Fig. 3: A few examples of stirrer configurations tested, with their case number referring to Table II. Each stirrer was based on dihedral elements, obtained by folding a 15×30 cm^2 copper plate, fixed between horizontal aluminium bars 22 cm distant. The overall dimensions are 38 cm wide and 66 cm high.

of a 90-degree folded 15×30 cm^2 copper plate. Copper was chosen in order to introduce negligible additional losses in the RCs and simplify comparisons. Table II describes the 33 configurations tested, divided according to the number of elements in the stirrer, from 6 to 1. Test case #34 corresponds to the stirrer stripped of all the elements, with just its central axis and the four horizontal aluminium bars to which the dihedral elements were fixed. It only served as a reference for later comparison in Secs. IV and VII. Fig. 3 shows eight examples of tested stirrers. All stirrers were tested in RC B, while only part of them were also tested in RC A and C, as described in Table I.

IV. Intrinsic Stirring Efficiency

The first eight stirrer configurations in Table II were tested in all three RCs, in order to confirm the prediction that τ_o and R_s are independent of the RC volume and losses. Fig. 4 compares the tACF of stirrer #1 at 1, 3 and 5 GHz, as a function of time normalized to each RC volume. The results clearly show that the normalization to the RC volume yields very similar results, which implicitly confirms that a stirrer moved from an RC of volume V_1 to a larger one of volume V_2 will present a stirring coherence time increased by a factor V_2/V_1. These results also show that the peak tACF, i.e., R_s, is practically unchanged across the three RCs.

An exponential regression was applied to the portion of tACF outside the shaded area, which represents the 95 % confidence interval of a zero correlation process estimated from a 100 sample population, as explained in Sec. III. The exponential regression, shown in Fig. 4 as a dashed black line, closely agrees with the tACF estimated in the three RCs and directly provides the stirrer coherence parameters R_s and τ_s,

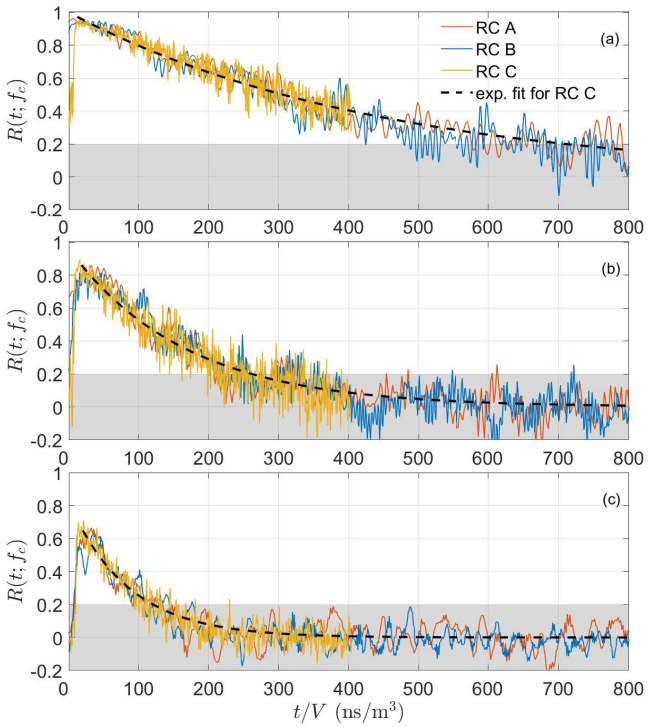

Fig. 4: Stirrer tACF for case #1 versus time normalized to the RC volume, for the three RCs described in Table I. Results estimated for f_c : (a) 1 GHz, (b) 3 GHz and (c) 5 GHz.

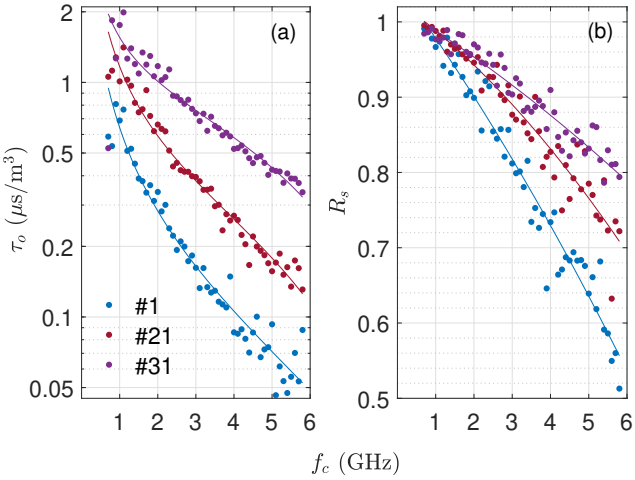

Fig. 5: ISEP estimated from the tACF of three different stirrers tested in RC B (circles), with their second-order polynomial regression results (solid lines).

with the intrinsic stirring coherence time τ_o readily found from (4).

Fig. 5 shows the resulting ISEP, i.e., R_s and τ_o, versus frequency for three stirrer configurations. It is apparent how these results are affected by a non-negligible uncertainty, in particular at the high-frequency end. The reason for this higher uncertainty is explained by the much faster exponential decay of the tACF, thus covering less time samples available for the exponential regression outside the shaded area, resulting in a higher sensitivity to statistical uncertainty in the tACF.

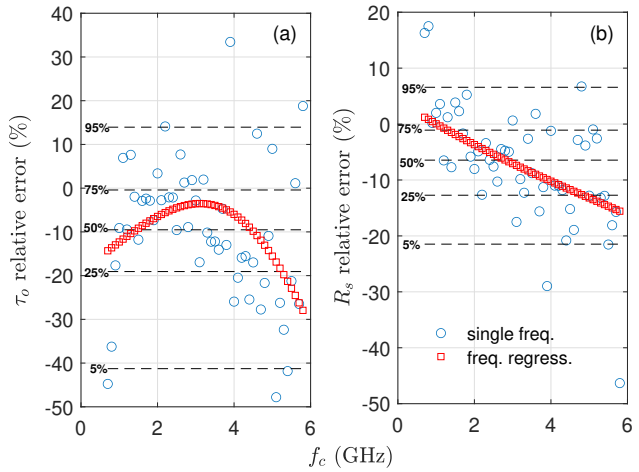

Fig. 6: Relative error between the ISEP of stirrer #1 estimated in RC B and C, for individual-frequency estimates and after polynomial regression across frequency (cf. Fig. 5). Quantiles for the distribution of relative errors for the single-frequency results are shown in the plots for reference.

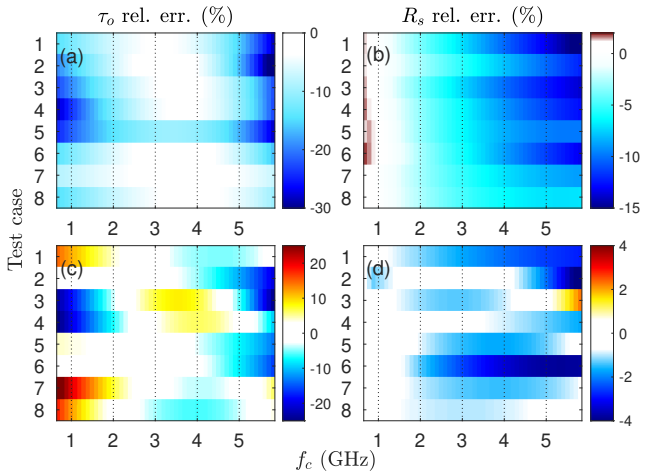

Fig. 7: Relative errors between estimates of τ_o (left column) and R_s (right column) obtained in RC B and those obtained in RC C (top row) and RC A (bottom row), after polynomial regression over individual-frequency results.

In order to reduce this uncertainty and avoid outliers biasing our analysis, a further regression was applied to the whole set of individual estimates across the entire frequency range. The results in Fig. 5(a) show that τ_o decreases with the frequency, with a large dynamic range covered between 0.7 to 6 GHz, as also confirmed in sec. V for all other stirrers. The regression was thus applied to $\tau_o f_c$, in order to work with a reduced dynamic range, whereas R_s spans a much more limited range. A second-order polynomial regression was thus applied to these two quantities, with results presented in Fig. 5.

These results show that reducing the number of elements in the stirrer from 6 (case #1) to 3 (#21) and 1 (#31) leads to a major change in τ_o as well as a reduction in R_s. As expected, R_s converges to one at low frequency, where none of these stirrers is able to introduce disorder in just a few interactions, as opposed to higher frequencies, as clear in Fig. 5(b). It is worth noticing how at 1 GHz, even though $R_s \simeq 1$ for the three stirrers, τ_o is consistently smaller for larger stirrers.

The effectiveness of the frequency regression in reducing outliers is fundamental when comparing estimates of the ISEP obtained in different RCs. Fig. 6(a) shows the relative error between estimates of τ_o for stirrer #1 tested in the RCs B and C. When comparing results obtained from individual frequency estimates, errors exceed ± 20 % with a 27 % probability, whereas when comparing τ_o estimates after frequency regression this probability is cut back to 9 %. Similarly for R_s, Fig. 6(b) shows a significant improvement in the relative error when frequency regression is applied, avoiding outlier-induced errors exceeding the 20 % threshold.

Fig. 7 extends the comparison of frequency-regressed results for stirrers #1-8 tested in the three RCs, comparing results obtained in RC B with those from the other two RCs. These results confirm that the errors are mostly within a 20 % bound for τ_o, while significantly better accuracy is observed for R_s.

In conclusion, the ISEP of the first eight stirrer cases estimated in the three RCs closely agree over the entire frequency range. Since similar results are obtained for RCs with different volume and losses, they support the claim that the ISEP are independent of the RC configuration.

V. Comparing Stirrer Efficiencies

Having tested all 33 stirrer configurations in RC B, their ISEP can be compared in order to understand their dependence on the number of elements in the stirrers and their relative orientation. The same procedure described in the previous section was applied, including frequency regression.

This comparison of stirrer configurations should by no means be regarded as a search for an optimal stirrer design. Such a goal would require exploring way more configurations with more degrees of freedom. We are rather seeking to show how the proposed ISEP are easier to compare since they are not biased by an RC volume and losses, making it possible to identify similarities and significant differences in the efficiency of the stirrer cases. Indeed, this section shows that τ_o is well-explained by simple physical phenomena known to be at the basis of mechanical stirrer efficiency, such as surface scattering.

Fig. 8(b) shows τ_o for the 33 stirrers tested, divided by dashed lines according to the number of dihedral elements, as detailed in Table II. It is apparent that τ_o abruptly increases when reducing the number of elements, while less pronounced differences are observed for configurations sharing the same number of elements. On the contrary, Fig. 8(a) shows a much smoother evolution of R_s, gradually increasing as the number of elements decreases, and presenting no dramatic reduction, spanning a range from 0.6 to 1.

This major difference in the pace of change of the two ISEP has direct practical implications. Indeed, as recalled in Sec. II, R_s is mostly important under heavy loading conditions, where τ_o has a minor impact. But as long as τ_a/V is not exceedingly smaller than τ_o, abrupt increments in the latter would lead to a

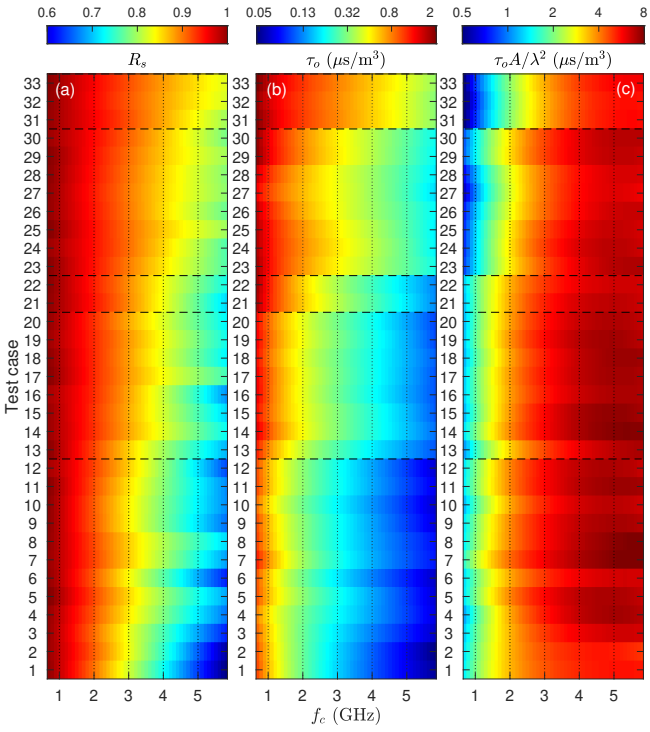

Fig. 8: ISEP estimated in RC B for the 33 stirrers tested, divided by dashed lines according to the number of dihedral elements, as described in Table II.

significant degradation of the stirrer efficiency, with the fACF increasing accordingly.

Therefore, we will focus on τ_o in the remained of this section. In order to better appreciate the differences in the stirrer efficiency, it would be useful to normalize the results according to a common physical criterion, in order to reduce the wide dynamic range of the results, spanning almost two orders of magnitude. It has been observed in the literature [5], [9], [31] that the dimensions of the stirrer has a major impact on its stirring efficiency, in particular, the stirrer external diameter and its projected height [1].

Based on these previous observations, we tested the hypothesis that the main physical phenomenon behind the efficiency of an electrically large stirrer is surface scattering. We thus expect τ_o to be inversely proportional to its electrical area A/λ^2. Normalizing τ_o accordingly leads to Fig. 8(c), where the relative variation across the stirrer configurations is now limited to less than 10 % above 3 GHz, where the dihedral elements are at least 1.5 wavelengths wide and therefore displaying a moderately directive scattering pattern. Only three outstanding cases feature better results, namely #1, #2 and #6, in stark contrast with #7 and #8.

These results provide a visual demonstration of the simpler comparison enabled by the ISEP, where it becomes much easier to highlight the role of the stirrer dimensions and the frequency and identify common physical mechanisms explaining an apparently very different performance. These results should be compared to the more complex procedures applied in the previous analysis, where it was less clear how different stirrer performances should be compared and most importantly not trivial to draw conclusions about which design parameters affect the stirrer efficiency [7], [9].

At frequencies below 2 GHz, surface scattering is expected to be less effective as a means of introducing disorder upon stirrer rotation, since the scattering pattern of each face of the dihedral elements would no longer be directive, thus generating a scattering less sensitive to stirrer rotation. Under these conditions edge diffraction from the dihedral elements can be expected to have an increasingly important role as the frequency decreases, explaining why the normalized $\tau_o A/\lambda^2$ is better, i.e., smaller, than at higher frequencies. For two- and single-element stirrers, $\tau_o A/\lambda^2$ is even lower, suggesting the existence of a further diffraction mechanism, which can be assumed to be the diffraction from the horizontal bars now free from dihedral elements. Confirming this tentative explanation will require further analysis, but seems compatible with the differences observed across the stirrer cases tested.

Thanks to the normalized results in Fig. 8(c) it is now easier to identify notable differences between the stirrers. Among six-element configurations (#1-12), for #1 and #2 τ_o decreases about 25 % faster at higher frequency, with #2 very similar to a common Z-fold stirrer design. Starting from #1 and rotating its right half by 45 and 90 degrees, leads to stirrers #3 and #4 respectively. Fig. 8(c) shows that this rotation results in a progressive loss of efficiency. A similar approach is applied row-wise to produce #5, resulting in a similar loss of efficiency.

Of special interest are the changes from #1 to #9 and from #2 to #12. Both pairs present the same change in structure, with the initial version presenting dihedral elements sharing the same planes, as visible in Fig. 3 for #2; the other configuration in each pair features a break in the stirrer surface area, with left and right halves no longer sharing the same planes, as in Fig. 3 for #12. In both cases, this change in the stirrer structure results in a 30 % increase of τ_o at high frequency, even though they share the same low-frequency behavior and initial coherence loss R_s. It seems reasonable to assume that this loss of efficiency is caused by their smaller contiguous surface, resulting in a less directive scattering and therefore lower sensitivity to the stirrer position. A loss of efficiency is also observed for #6 to #8, compared to #1, which share a more complex structure with an even lower contiguous surface.

Among configurations with four and three elements no major difference was observed, with a 10 % maximum difference in τ_o, with several configurations derived from six-element stirrers by removing a row of elements. No notable difference was either found among two- and single-element stirrers. The former group explored different combinations depending only on the dihedral positions, from a row at three different distances from the RC ceiling (#23-25), to having them aligned vertically (#26-27) or non-adjacent (#28-30). Only the vertically aligned cases present a minor 10 % improvement.

Results for #34, where all dihedral elements were removed, are not shown in Fig. 8, since τ_o would be out of scale

[1] i.e., observed orthogonally to the stirrer rotation axis

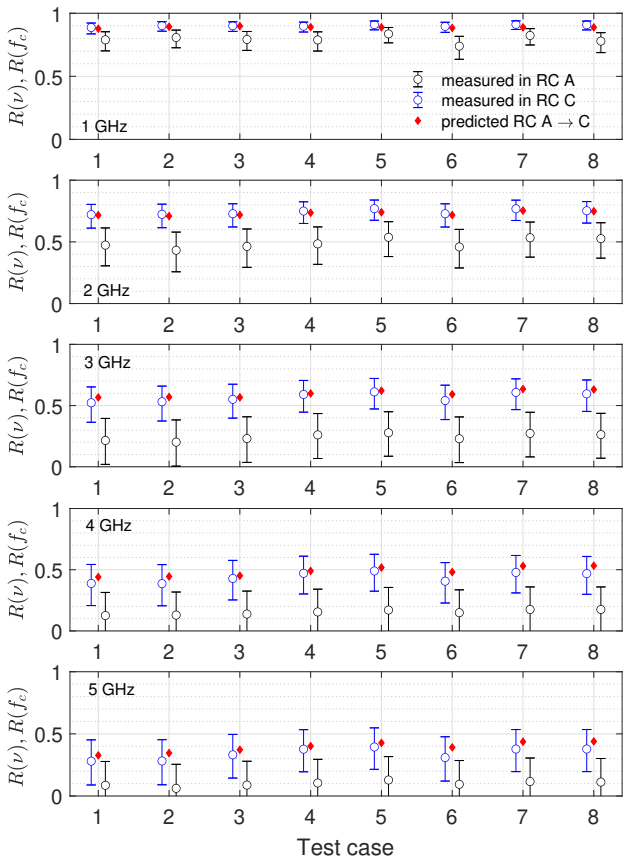

Fig. 9: Comparison between the fACF estimated in RC A and C for the stirrers #1-8, and the fACF in RC C predicted from data collected in RC A. Uncertainty bars are slightly offset around each frequency for ease of comparison.

compared to the other results. In this case R_s is equal to 1 below 1 GHz and 0.85 at best at 5.8 GHz, whereas τ_o is 70 % higher than #33 below 1 GHz and 280 % higher above 3 GHz. These last results imply that the horizontal bars have a non-negligible, though not dominant, role compared to #33 at low frequency, where the stirrer electrical area is negligible, while above 3 GHz they have no effect on the stirring efficiency, thus supporting our earlier interpretation of the low-frequency behavior of τ_o being explained by edge diffraction.

These results show how the ISEP provide a finer access to stirring efficiency information, with a wide dynamic range for τ_o that could not be suspected from the fACF. Indeed, the fACF is bound to less than one order of magnitude, with values below 0.1 hardly observed, as shown in the next two sections. Thanks to τ_o it is also possible to clearly observe how the stirring efficiency evolves over frequency, independently of the RC characteristics, as opposed to the fACF, as discussed in Sec. VII. Furthermore, the fact that τ_o is well explained by the electric surface area of the stirrer, as long as it is wider than 1.5 wavelengths, is of particular interest, providing quantitative evidence of this property that was not clearly confirmed in the literature.

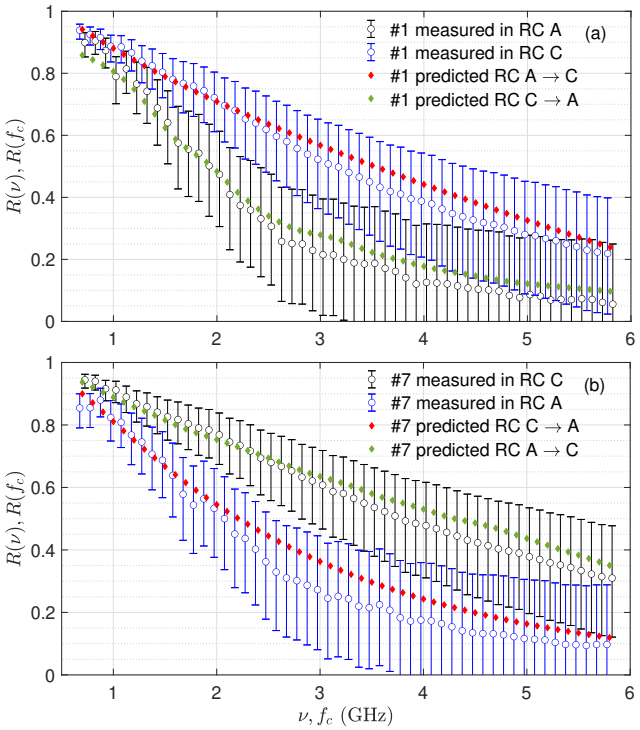

Fig. 10: Comparison between the fACF versus frequency estimated in RC A and C and the fACF predicted for RC A from data collected in RC C and viceversa, for (a) stirrer #1 and (b) #7.

VI. Predicting Stirrer Efficiency in a Different RC

A major advantage of the RC-independence of the ISEP is the possibility to predict how a given stirrer would perform in another RC, without having to test it first-hand. Eq. (3) establishes that it is only necessary to know a stirrer ISEP, the target RC volume and its expected power-decay time.

Having tested the first eight stirrers in Table II in all of the three RCs, it is possible to directly verify the accuracy of the fACF predicted thanks to the ISEP. Fig. 9 presents the fACF measured in RC A and RC C for these stirrers, from 1 to 5 GHz. Confidence intervals are shown for each estimate, calculated for a 95 % confidence for a population of 100 samples, according to Fisher approximation [29]. A remarkable loss of stirrer efficiency can be noticed, in line with the observations reported in [9] about the negative impact of a larger RC on the stirring efficiency of a mechanical stirrer.

Fig. 9 also shows the fACF in RC C predicted from the stirrer's ISEP estimated in RC A, having used the power-decay time estimated from the empty RC C. A very good agreement is found across all eight stirrers over the entire frequency range.

These results prove that the proposed procedure can accurately predict a stirrer efficiency in an RC, starting from its ISEP estimated in another RC of significantly different dimensions: as detailed in Table I, RC C is about 18 times larger than RC A, where the ISEP of the eight stirrers were estimated. As argued in Sec. VII, the notable loss of stirring

efficiency of these stirrers in RC C, compared to RC A, is caused by its higher losses, and not by an hypothetical insufficient efficiency of the stirrer design.

The prediction accuracy of (3) can be better appreciated in Fig. 10(a), where the measured and predicted fACF for #1 are shown as a function of frequency. It can be observed how the slope of the fACF measured in RC A is predicted by (3) to dramatically change when moving the stirrers to RC C, and viceversa when predicting the fACF in RC A based on the ISEP estimated in RC C. A good agreement is observed between measured and predicted fACF in both configurations. In particular, it is remarkable that the relatively highly correlated results in RC C, once processed to extract the stirrer ISEP, can predict the significant improvement of the fACF of these stirrers when installed in the much smaller RC A.

The different slopes of the fACF for RC A and C are explained by the different power loss mechanisms in the aluminium and steel RCs, with dissipation in aluminium surfaces yielding a partial quality factor scaling as $\sqrt{\nu}$ [32], whereas for galvannealed (and galvanized) steel plates it rather scales as ν [33]. Similar conclusions can be drawn from results in Fig. 10(b), where stirrer #7 was considered.

Given the different frequency dependence of the these two RCs, these results confirm that the fACF provides a partial and biased measure of the role of a stirrer design in the stirring efficiency, with RC losses heavily contributing to the fACF. An unbiased information is instead ensured by the ISEP, allowing to draw more robust conclusions about the stirrer efficiency over a wide frequency range.

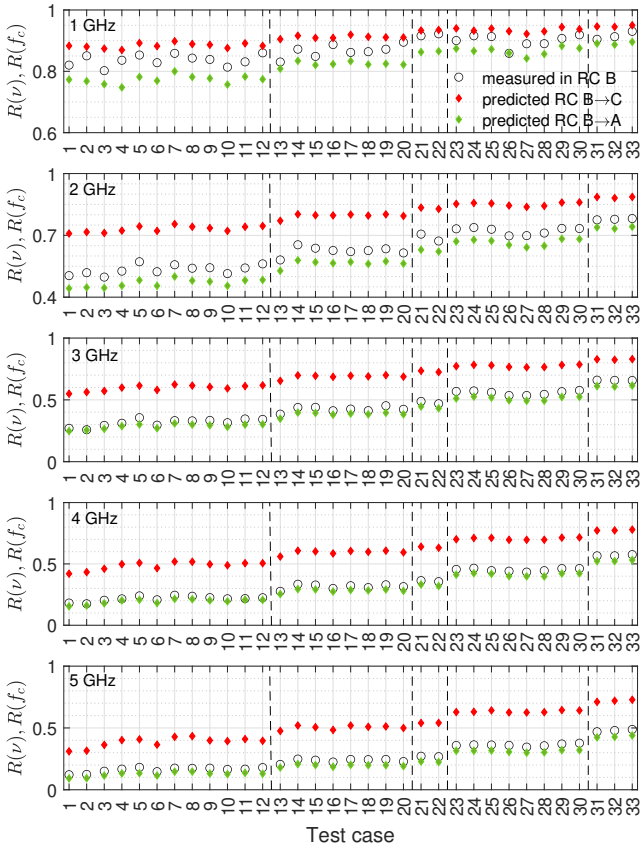

Fig. 11: Predicted fACF for RC A and C, based on data collected in RC B for all stirrer configurations.

VII. Selecting a Stirrer for a Target Efficiency

As observed in the previous section, using the same stirrer in two RCs with a significant different volume does not result in the same fACF. This would happen only for the special case where the RCs share similar volume-to-metal-surface ratios and wall conductivities, resulting in identical τ_a/V and therefore the same fACF for both RCs, as required by (3).

In general this condition is not met. The question, fundamental in RC design, is how a stirrer for a new RC should be selected in order to ensure a target fACF, without having to run multiple tests with different candidate stirrers in the new RC.

If a satisfying stirrer design is known and previously tested and validated in an RC of volume V and decay time τ_a, it would be very practical to know how the same stirrer should be adapted to another RC of volume V' and expected decay time τ_a'. Eq. (3) provides part of the answer to this question, since enforcing the same fACF for the two RCs requires

$$\frac{\tau_o'}{\tau_o} \simeq \frac{\tau_a'}{V'}\frac{V}{\tau_a} \tag{5}$$

since $R_s \simeq R_s'$, as shown in sec. V. This result provides a simple guideline about how τ_o' in the new RC should be scaled in order to make up for higher losses.

Once the new stirrer's τ_o' is known, two paths are available: either selecting a stirrer design among a set of already known models, such that it has an intrinsic stirring coherence time close to the target τ_o'; or scaling the initially tested stirrer in order to modify its τ_o and tune it to the new RC where τ_o' is required. The first approach may call for a different stirrer design, whereas the second would only apply a scaling factor. For this last choice, it was observed in Sec. IV that as soon as the stirrer surface area A covers more than two square wavelengths $\tau_o \sim \lambda^2/A$. Hence,

$$A/A' \simeq \tau_o'/\tau_o. \tag{6}$$

In case power loss were mainly due to dissipation in an RC walls, $Q \simeq 1.5V/S_w\delta$ [32], with S_w the RC boundary surface area and δ the skin-effect depth, (6) yields

$$A/S_w \simeq A'/S_w' \tag{7}$$

for walls of same conductivity, with the stirrer surface area thus scaling with the RC wall's. We did not have the opportunity to experimentally confirm this prediction, since it would have called for the manufacturing of multiple stirrers of ad hoc dimensions. It is worth reminding that multiple loss phenomena can contribute to an RC decay time, so a more complex dependence on the RC feature should be expected, depending on the targeted frequency range.

Instead, we took advantage of the small library of 33 stirrers tested with RC B in Sec. IV, in order to verify that the ISEP can help selecting the stirrer for two different RCs in order to ensure the same fACF, and therefore the same stirring efficiency. To this end (3) was applied to the stirrer parameters

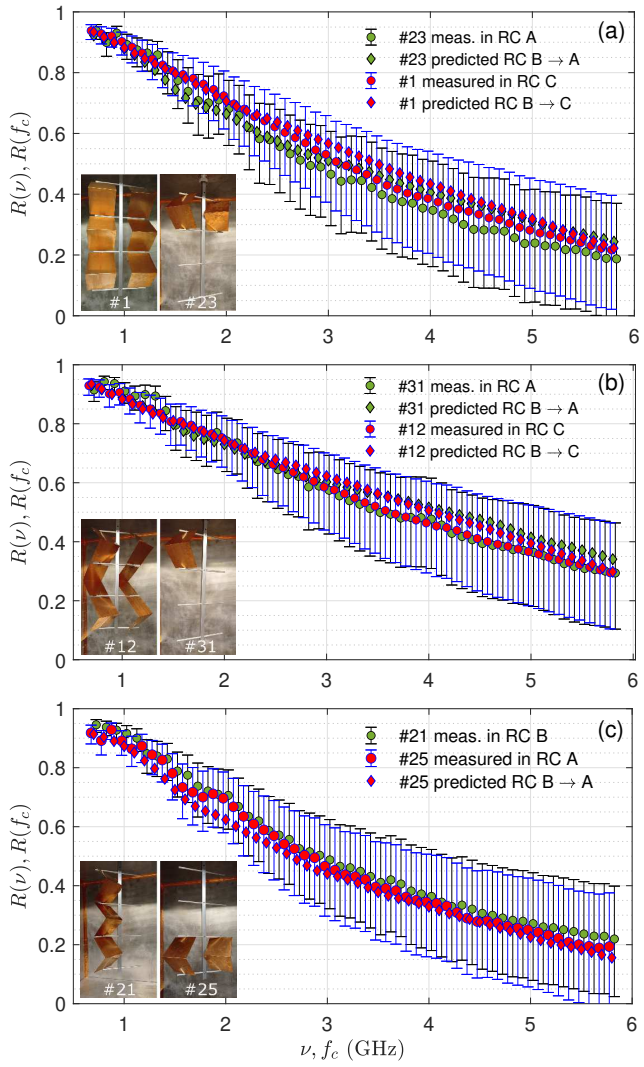

Fig. 12: Measured and predicted results (from RC B) for three examples where the same fACF is required in two different RCs. For each example the two stirrer designs predicted to meet the required fACF are shown in the inset picture.

estimated in RC B to predict their fACF in RC A and C as targets, yielding the results in Fig. 11. Comparing the results for RC A and C, it appears that there exist several pairs of stirrer configurations predicted to provide similar fACF in these two RCs.

Three such pairs were selected. The first one is stirrer #1 for RC C and #23 for RC A, which can be seen in the inset in Fig. 12(a) to have six and two dihedral elements, respectively. Hence, τ_o for #1 is about three times larger then #23, as confirmed in Fig. 8(b), while their R_s differ by less than 30 % in Fig. 8(a). The fACF measured for these two stirrers in their respective RCs are shown in Fig. 12(a) to closely agree, as well as the fACF predicted from the stirrers' ISEP estimated in RC B, with a maximum error below 20 %.

The second stirrer pair tested involved stirrer #12 for RC C and #31 for RC A. The results in Fig. 11 predict that the fACF should be slightly higher than with the previous stirrer pair. Fig. 12(b) confirms that the fACF is indeed measurably higher, with the fACF observed in RC A and RC C agreeing with the one predicted from RC B.

A third comparison involved RCs A and B, with stirrer #25 tested in RC A and #21 in RC B. The stirrer surface areas now differ by a factor 50 % only, reflecting the more limited change in RC volume and losses compared to the two previous cases. Since RC A and B have the same wall conductivity, (7) requires that the increase of stirrer surface area increases by the ratio of the wall surface area of the two RC, which is found in Table I to be equal to 62 %. This result is very close to the 50 % increase in the stirrer surface areas. Also in this case the predicted similarity in fACF was confirmed by the results in Fig. 12(c).

These results confirm two important points: first, that the stirrer ISEP can be effectively used to predict how a stirrer would perform in a different RC. The similarity in the fACF shown in Fig. 12 should be compared to the significant difference in fACF observed in Fig. 10, when the same stirrer was tested in different RCs. Second, the difference in volume, and therefore losses, between the three RCs calls for different stirrer dimensions if the same fACF is required. The significantly larger stirrers needed in RC C are essentially a consequence of higher surface losses on its walls.

VIII. Conclusions

This paper has proven that it is possible to estimate the efficiency of a mechanical stirrer independently of the reverberation chamber (RC) where it is tested. Two intrinsic stirrer efficiency parameters (ISEP), τ_o and R_s, were shown to be RC independent and can be used to accurately predict the stirrer efficiency in other RCs, as measured by the frequency-domain auto-correlation function (fACF) of field-related quantities.

These results are of practical important for RC users, as they show that it is not necessary to build multiple stirrer prototypes and undergo time-consuming tests in order to ensure a satisfying stirring efficiency in an RC. If the ISEP of a collection of stirrers are available, it is possible to simply and quickly predict which stirrer design provides the best performance in terms of stirring efficiency versus geometrical dimensions. Moreover, the stirrer parameters can be estimated in different RCs, with no need to run tests necessarily in the same RC, thus enabling collecting stirring parameters across a wider range of different experimental tests, instead of being limited by those obtained in a single RC setup.

Another important result is the confirmation that the stirring efficiency measured by means of their fACF is heavily influenced by the RC volume and losses. There are two implications here: on the one hand, attempting to identify universal design rules for stirrers through comparison of their fACF will necessarily result in biased conclusions, as the same stirrer would perform differently in another RC; on the other hand, the proposed stirrer efficiency model predicts that as a larger RC is used, the stirrer needs to have a lower τ_o, which was here shown to require it to be electrically larger. This last point essentially explains in simple and quantitative terms why larger stirrers are needed in larger RCs, in order to ensure the same stirring efficiency, independently of the need to extend

their range of operation to the lower frequencies warranted by the larger RC dimensions.

REFERENCES

[1] R. Serra, A. C. Marvin, F. Moglie, V. M. Primiani, A. Cozza, L. R. Arnaut, Y. Huang, M. O. Hatfield, M. Klingler, and F. Leferink, "Reverberation chambers a la carte: An overview of the different mode-stirring techniques," *IEEE Electromagn. Compat. Magazine*, vol. 6, no. 1, pp. 63–78, First 2017.

[2] *Testing and measurement techniques - Reverberation chamber test methods*, International Electrotechnical Commission (IEC) Std. 61 000-4-21, 2011.

[3] *Environmental Conditions and Test Procedures for Airborne Equipment*, Radio Technical Commission for Aeronautics (RTCA) Std. DO-160G, 2014.

[4] R. Serra, "Reverberation chambers through the magnifying glass: an overview and classification of performance indicators," *IEEE Electromagn. Compat. Mag.*, vol. 6, no. 2, pp. 76–88, 2017.

[5] D. Wu and D. Chang, "The effect of an electrically large stirrer in a mode-stirred chamber," *IEEE Trans. Electromagn. Compat.*, vol. 31, no. 2, pp. 164–169, 1989.

[6] O. Lundén and M. Bäckström, "Stirrer efficiency in FOA reverberation chambers. evaluation of correlation coefficients and chi-squared tests," in *IEEE Intern. Symp. Electromagn. Compat.. Symposium Record*, vol. 1, 2000, pp. 11–16 vol.1.

[7] J. Clegg, A. Marvin, J. Dawson, and S. Porter, "Optimization of stirrer designs in a reverberation chamber," *IEEE Trans. Electromagn. Compat.*, vol. 47, no. 4, pp. 824–832, 2005.

[8] P. Hallbjörner, "A model for the number of independent samples in reverberation chambers," *Microwave and optical technology letters*, vol. 33, no. 1, pp. 25–28, 2002.

[9] N. Wellander, O. Lundén, and M. Bäckström, "Experimental investigation and mathematical modeling of design parameters for efficient stirrers in mode-stirred reverberation chambers," *IEEE Trans. Electromagn. Compat.*, vol. 49, no. 1, pp. 94 –103, feb. 2007.

[10] A. Ubin, R. Vogt-Ardatjew, F. Leferink, M. Z. Mohd Jenu, and S. Van De Beek, "Statistical analysis of three different stirrer designs in a reverberation chamber," in *2015 Asia-Pacific Symp. Electromagn. Compat. (APEMC)*, 2015, pp. 604–607.

[11] F. Moglie and V. M. Primiani, "Reverberation chambers: Full 3D FDTD simulations and measurements of independent positions of the stirrers," in *2011 IEEE Intern. Symp. Electromagn. Compat.*, 2011, pp. 226–230.

[12] Y. Huang, J. T. Zhang, and P. Liu, "A novel method to examine the effectiveness of a stirrer," in *2005 Inter. Symp. on Electromagn. Compat., 2005*, vol. 2, 2005, pp. 556–561.

[13] J.-I. Hong and C.-S. Huh, "Optimization of stirrer with various parameters in reverberation chamber," *Progress In Electromagnetics Research*, vol. 104, pp. 15–30, 2010.

[14] L. Arnaut, "Effect of size, orientation, and eccentricity of mode stirrers on their performance in reverberation chambers," *IEEE Trans. Electromagn. Compat.*, vol. 48, no. 3, pp. 600–602, 2006.

[15] D. Fedeli, M. Iualè, V. M. Primiani, and F. Moglie, "Experimental and numerical analysis of a carousel stirrer for reverberation chambers," in *2012 IEEE Intern. Symp. Electromagn. Compat.*, 2012, pp. 228–233.

[16] Y. Huang, N. Abumustafa, Q. G. Wang, and X. Zhu, "Comparison of two stirrer designs for a new reverberation chamber," in *The 2006 4th Asia-Pacific Conference on Environmental Electromagnetics*, 2006, pp. 450–453.

[17] V. Creta, L. Bastianelli, F. Moglie, V. M. Primiani, and L. R. Arnaut, "Stirring performance of helically distributed paddles," in *2017 IEEE Intern. Symp. Electromagn. Compat. & Signal/Power Integrity (EMCSI)*, 2017, pp. 670–674.

[18] J. Tang, F. Li, J. Zheng, X. Chen, Y. Li, and J. Chen, "A new mode stirrer design for the reverberation chamber," *The Applied Computational Electromagnetics Society Journal (ACES)*, pp. 1182–1188, 2021.

[19] X. Chen, "On independent platform sample number for reverberation chamber measurements," *IEEE Trans. Electromagn. Compat.*, vol. 54, no. 6, pp. 1306–1309, 2012.

[20] A. Adardour, G. Andrieu, and A. Reineix, "Determination of the "quasi-ideal reverberation chamber minimal frequency" according to loading," in *2013 IEEE Intern. Symp. Electromagn. Compat.*, 2013, pp. 213–216.

[21] F. Moglie and V. M. Primiani, "Analysis of the independent positions of reverberation chamber stirrers as a function of their operating conditions," *IEEE Trans. Electromagn. Compat.*, vol. 53, no. 2, pp. 288–295, 2011.

[22] R. J. Pirkl, K. A. Remley, and C. S. L. Patané, "Reverberation chamber measurement correlation," *IEEE Trans. Electromagn. Compat.*, vol. 54, no. 3, pp. 533–545, 2012.

[23] V. Rajamani, C. F. Bunting, and J. C. West, "Effects of loading on independent samples and uniformity of a reverberation chamber," in *2013 IEEE Intern. Symp. Electromagn. Compat.*, 2013, pp. 217–221.

[24] X. Chen, "Experimental investigation of the number of independent samples and the measurement uncertainty in a reverberation chamber," *IEEE Trans. Electromagn. Compat.*, vol. 55, no. 5, pp. 816–824, 2013.

[25] G. Andrieu, N. Ticaud, F. Lescoat, and L. Trougnou, "Fast and accurate assessment of the "well stirred condition" of a reverberation chamber from S_{11} measurements," *IEEE Trans. Electromagn. Compat.*, vol. 61, no. 4, pp. 974–982, 2019.

[26] G. Esposito, G. Gradoni, F. Moglie, and V. M. Primiani, "Stirrer performance of reverberation chambers evaluated by time domain fidelity," in *2013 IEEE Inter. Symp. on Electromagn. Compat.* IEEE, 2013, pp. 207–212.

[27] A. Cozza, "Stirring coherence time to predict stirrer efficiency in loaded reverberation chambers," *IEEE Trans. Electromagn. Compat.*, vol. 66, no. 1, pp. 37–48, 2024.

[28] Q. Xu, Y. Huang, L. Xing, Z. Tian, C. Song, and M. Stanley, "The limit of the total scattering cross section of electrically large stirrers in a reverberation chamber," *IEEE Trans. Electromagn. Compat.*, vol. 58, no. 2, pp. 623–626, 2016.

[29] N. J. Salkind, *Encyclopedia of measurement and statistics*. SAGE publications, London, 2006.

[30] C. L. Holloway, H. A. Shah, R. J. Pirkl, K. A. Remley, D. A. Hill, and J. Ladbury, "Early time behavior in reverberation chambers and its effect on the relationships between coherence bandwidth, chamber decay time, rms delay spread, and the chamber buildup time," *IEEE Trans. Electromagn. Compat.*, vol. 54, no. 4, pp. 714–725, Aug 2012.

[31] O. Lundén, N. Wellander, and M. Bäckström, "Stirrer blade separation experiment in reverberation chambers," in *2010 IEEE Inter. Symp. on Electromagn. Compat.*, 2010, pp. 526–529.

[32] D. A. Hill, *Electromagnetic fields in cavities: deterministic and statistical theories*. John Wiley & Sons, 2009.

[33] A. Cozza and F. Monsef, "Power dissipation in reverberation chamber metallic surfaces based on ferrous materials," *IEEE Trans. Electromagn. Compat.*, vol. 61, no. 6, pp. 1714–1725, 2018.

Andrea Cozza (S'02 - M'05 - S'12) received the Laurea degree (summa cum laude) in electronic engineering from Politecnico di Torino, Turin, Italy, in 2001 and the Ph.D. degree in electronics engineering jointly from Politecnico di Torino and University of Lille, France, in 2005. In 2007, he joined SUPELEC (now CentraleSupelec), Gif sur Yvette, France, where since 2013 he is Full Professor. He conducts his research activities at GeePs, the Group of Electrical Engineering of Paris, Gif sur Yvette, France. His current research interests include reverberation chambers, statistical electromagnetics, wave propagation through complex media, fault location techniques in transmission lines and applications of time reversal to electromagnetics. Mr. Cozza's awards and honors include the 2012 Prix Coron-Thévenet (Académie des Sciences) and the 2019 Richard B. Schulz Best Transaction Paper Award (IEEE Transactions on Electromagnetic Compatibility).